

Microwave ionization of Rb Rydberg atoms: Frequency dependence

L. Sirko,* M. Arndt, P. M. Koch,[†] and H. Walther

*Sektion Physik, Universität München, D-85748 Garching, Germany
and Max-Planck-Institut für Quantenoptik, D-85748 Garching, Germany*

(Received 21 July 1993; revised manuscript received 28 October 1993)

We report on an experimental study of the frequency dependence of the microwave “ionization” probability for laser-excited $\text{Rb}(np)^2P_{3/2}(|M_J|=\frac{1}{2})$ Rydberg atoms. Most data are for $n=84$. The microwave field was produced by a low-noise frequency synthesizer, and the laser-excited atoms subsequently driven by microwaves were kept in an environment cooled to 77 K in order to minimize the perturbing effects of the thermal, blackbody-radiation field. The driving frequency covered 4–14-MHz intervals around three frequencies between 8.87 and 16.14 GHz. Data are shown for 1- and 5- μs interaction times, which correspond to the driving frequency being resolved by the atoms to about 1 and 0.2 MHz, respectively. The turnon and turnoff parts of the microwave pulse shape were slow, lasting about 6 ns (*circa* 70 field oscillations). For the narrow frequency intervals used, the microwave field amplitude was calibrated *in situ* with use of two-photon Rabi-nutation measurements, which also directly demonstrated the spatial uniformity of the driving field amplitude and its coherence over at least a 1- μs time scale. Within the frequency intervals studied experimentally, we have observed no sharp, frequency-dependent structure outside of that expected from experimental counting statistics. We give physical arguments based on experimental data and previous experimental and theoretical work on microwave “ionization” that show that the present experiments have been in the range of the scaled frequency above 1. Thus, these experimental data examine in a continuous fashion the frequency dependence of microwave “ionization” in the high-scaled-frequency regime. Finally, we discuss our results in the light of published theoretical discussions of what might be expected to be the frequency dependence of the microwave “ionization” probability for various quantal models for the one-dimensional hydrogen atom in this high-frequency regime.

PACS number(s): 32.80.Rm, 03.65.-w, 72.20.-i

I. INTRODUCTION

Since its experimental discovery with hydrogen atoms [1] in 1974, the microwave ionization of highly excited (Rydberg) atoms has developed into an important vehicle for the study of the multiphoton ionization of atoms by strong oscillatory electric fields. Here, *strong* means that the driving field is not negligible compared to the Coulomb field binding the electron in its initial state. Because of the strong driving field and the large number of microwave photons energetically required for ionization, ranging from several tens to several hundreds or more, and the often high density of strongly coupled atomic states, quantal time-dependent perturbation theory has seldom been of practical use for calculating and understanding the important details of this physical process. However, its deficiency has furnished an impetus for the development of new theoretical methods for the treatment of this physical process; examples range from classical and semiclassical methods, to large numerical integrations of the time-dependent Schrödinger equation, to “dynamical localization theory” methods inspired by and somewhat related to those used in the theory of spatially

solid-state systems perturbed by extrinsic “disorder.” For the dynamical localization theory, however, the dynamics is deterministic; there are no random elements put in “by hand.”

Part of the richness of the microwave ionization process stems from the number of parameters that affect the evolution of the atom in the strong driving field and which may, in principle, be varied. These parameters include those needed to describe the particular atom being studied, e.g., the quantum numbers for the initial state and, if required by experimental conditions, those for a higher-lying state(s), the so-called “cutoff” state(s). If microwave excitation to states above the cutoff state(s) produces a signal essentially indistinguishable from “true” ionization—excitation to the zero-field continuum—then this cutoff contribution must be modeled for any comparison of theoretical results with experimental data for “ionization,” which denotes the sum of true ionization and excitation above the cutoff. Moreover, if the cutoff is varied experimentally [2], one gains some information about final population distribution among the bound states.

The parameters also include those needed to describe the oscillatory field, e.g., its angular frequency ω , electric amplitude F , and polarization, all as a function of time, in general. For shorthand we shall refer to the amplitude envelope function $F(t)$ as the pulse shape. If other external fields such as a static electric field, a second monochromatic, oscillatory field, or “noise” fields are present,

*Permanent address: Institute of Physics, Polish Academy of Sciences, Al. Lotników 32/46, 02-668 Warszawa, Poland.

[†]Permanent address: Physics Department, State University of New York, Stony Brook, NY 11794-3800.

e.g., the thermal, blackbody-radiation field, amplitude, or phase jitter on the oscillatory field itself, the parameters describing them must also be specified.

Because the two problems are described by essentially the same Hamiltonian, the comments in the preceding paragraph about the microwave “ionization” of Rydberg atoms also apply to (single-electron) multiphoton ionization and the so-called *above-threshold ionization* (ATI) of atoms by intense, pulsed-laser fields, as long as the process remains nonrelativistic.

To vary all these parameters in a controlled way is a formidable (if not tedious) experimental challenge for both kinds of experiments. Usually because of constraints imposed by the experimental apparatus, most experiments to date have varied only a small number of these parameters. Focusing on the microwave “ionization” process, physical intuition based on some limited data, coupled with various theoretical calculations or estimates, indicate that one should study closely how the “ionization” probability varies continuously with ω and the duration T and shape of “low-noise” microwave pulses. Because microwave technology is generally more accessible for wider variations than is short, intense-pulse laser technology, such microwave experiments are relatively more feasible.

Nevertheless, there have been few microwave “ionization” experiments in which the applied frequency was varied continuously. Bayfield, Gardner, and Koch [3] exposed hydrogen atoms with each principal quantum number n_0 in the range 45–57 to *circa* 10^2 oscillations of a microwave field varied between about 9.4–11.6 GHz in an X-band waveguide. Though the frequency was slowly and, for signal-averaging purposes, repetitively swept continuously in that experiment [3], the published experimental data were binned into about 12 frequency intervals in the above range. This was reasonable because each atom saw a microwave train whose frequency was resolved to only something like $1/10^2=1\%$. This transit-time limited frequency resolution of about 0.1 GHz was comparable to the bin width of about 0.15 GHz. To resolve the frequency more highly, it would be necessary to expose the atoms to more field oscillations. Nevertheless, even with this 1% frequency resolution, the data reported by Bayfield, Gardner, and Koch [3] exhibited resonant structure as a function of frequency for most of the values of n_0 that were studied.

It is useful to point out that the frequencies at which there were local minima (separated by about 2 GHz) in the “ionization” probability [3]—such minima mean there is local stability—were later [4,5] shown to be consistent with the physical origin of the variations reported by van Leeuwen *et al.* [6] of the dependence of the scaled threshold amplitudes $n_0^4 F(10\%)$ for 10%–“ionization” probability on a stepwise variation of the scaled frequency $n_0^3 \omega$. A classical explanation for these observed variations [6] linked the local stability near certain low-order rational values of $n_0^3 \omega$ with the stabilizing influence of nonlinear trapping resonances in the classical phase space. These are only one example of a variety of resonance phenomena [5,7] that have been found in the microwave “ionization” of hydrogen atoms.

The hydrogen-atom experiments of Koch and co-workers [7] have concentrated on studying the dependence of the microwave “ionization” probability for stepwise variations of the *scaled frequency* $n_0^3 \omega$ over a large range. Such experiments have used various fixed frequencies of resonant cavities between $\omega/2\pi=7.58$ and 36.02 GHz and values of n_0 between about 24–90. An advantage is the very large dynamic range of $n_0^3 \omega$ that has been covered, about 150; a disadvantage is that it has not been covered continuously.

The helium-atom experiments [8] carried out with the same apparatus have used triplet nS states exposed to a microwave frequency that, thus far, has always been much smaller than the frequency splitting between the initial n shell and its immediate neighbors. In this sense, these experiments have covered only low scaled frequencies.

The recent hydrogen-atom experiment of Bayfield and co-workers [9–12] has used waveguide interaction regions that permit the frequency to be varied continuously over the usable bandwidth of the waveguide, typically about 50%, but their published data for continuous variation of the frequency have concentrated on microwave amplitudes below those at which microwave “ionization” sets in. Graphs showing the frequency dependence of the probability for some n -changing transitions may be found in Refs. [10–12]. The microwave “ionization” data from this group have covered in a stepwise fashion the scaled-frequency range between about 0.2–2.6.

The alkali-metal and alkaline-earth-metal Rydberg-atom experiments of Gallagher [13] have been carried out for n states at several discrete microwave frequencies that were less—often significantly less—than the frequency splitting between the initial n shell and its neighbors. In this sense, these experiments have covered in a stepwise fashion only scaled frequencies below 1.

In various ranges of the scaled frequency, different numerical calculations have indicated that one might expect to see appreciable variation at a fixed microwave amplitude of the microwave “ionization” probability as the frequency is varied. Blümel and Smilansky ([14], see Fig. 6) found structure on a few-MHz scale around 9.80 GHz when they numerically integrated the time-dependent Schrödinger equation for a one-dimensional hydrogen atom initially in the $n_0=36$ level. Their investigated frequency interval covered a narrow range of rather low scaled frequencies near $n_0^3 \omega=0.07$. They explained both this frequency-dependent structure and an amplitude-dependent structure as well [14,15] via state-mixing effects near avoided crossings of Floquet (quasienergy) potential curves.

With use of the *quantum-Kepler map*, which is a model for the periodically driven, one-dimensional hydrogen atom that is based on the quantized version of a discretized, classical, Kepler-orbital-return map, Casati, Guarneri, and Shepelyansky [16] investigated the frequency dependence of the microwave “ionization” probability for some intervals of scaled frequency not too far above 1. They found huge fluctuations that persisted down to a scale of fractional variation in the frequency of 10^{-6} . The physical reason for the fluctuations was traced to the

“pseudorandom” nature of frequency detunings [16].

Leopold and Richards [17] compared solutions of the iterated quantum-Kepler map with those obtained from the continuous flow of the time-dependent Schrödinger equation for a one-dimensional hydrogen atom. They concluded that the fluctuations on such a fine frequency scale were an artifact of the map; this will be discussed further in Sec. V. However, their solutions of the time-dependent Schrödinger equation [17,18] did exhibit noticeable fluctuations in the microwave “ionization” probability over frequency intervals $\Delta\omega/\omega$ of a percent or so, whose origin was linked theoretically to the erratic, but deterministic, behavior of frequency-detuning parameters as the driving frequency (or other experimental parameters such as a superimposed static electric field) was varied in the calculations. Additional numerical studies of the frequency dependence of the solutions of the time-dependent Schrödinger equation are underway [19].

These introductory comments serve to point out that careful experimental studies of the frequency dependence of the microwave “ionization” of Rydberg atoms are called for. This paper reports results of an experimental survey carried out with Rb Rydberg atoms. The frequency dependence of microwave “ionization” for scaled frequencies exceeding 1 is examined for driving frequencies *circa* 10^{10} Hz with a frequency resolution at or below the 1 MHz range.

The paper is organized as follows. Section I presents the Introduction. Section II describes the experimental method, contrasting it with other experimental methods used in previous microwave “ionization” studies. Section III presents in graphical form our experimental data. Section IV presents a brief discussion of these data. Section V concludes with an interpretation of the experimental results, as far as it is possible, in terms of previously published theoretical discussions of the frequency dependence for microwave “ionization” and an analogy drawn between this process and that of “conductance fluctuations” in mesoscopic, solid-state systems.

II. EXPERIMENTAL METHOD

“Ionization” experiments with excited hydrogen [1–3,6,7,9–12,20–24] and helium [8,25] Rydberg atoms interacting with strong microwave fields in a cavity or waveguide have been carried out using fast atomic beams in the 10–20-keV range. This method [26] uses collisionally excited, low-lying ($n=7$) Rydberg Stark states that are subsequently excited via $n=9$ or 10 Stark states to high-lying ($n \geq 24$) Stark states, with infrared radiation from continuous CO_2 lasers being used for each transition step. Because the atoms fly at a high and uniform speed through the apparatus, various spatially separated regions of laser, static, or microwave fields are experienced in the moving, inertial atomic frame as a series of temporal events. This has the advantage of the temporal sequence being very reproducible for each atom in the fast beam (low pulse-to-pulse jitter); it has the disadvantage of making it somewhat difficult to vary widely the interaction time with, e.g., the microwave field, while keeping the interactions with the other fields used for, e.g.,

atomic-state preparation, fixed. Moreover, because the typical time-of-flight through a few-meter-long vacuum apparatus is only a few microseconds, interaction times with the microwave field have been (well) below the microsecond range with this method.

Because of the availability of tunable laser sources that are well matched to their energy level spacings, microwave “ionization” experiments with alkali-metal and alkaline-earth-metal atoms are more conveniently carried out in thermal beams. In a series of experiments Gallagher and co-workers [13,27–31] have used pulsed visible-laser, stepwise excitation of Li, Na, K, and Ba atoms to study the interactions of their Rydberg states with pulses of microwave fields in cavities resonating at a few frequencies between about 9–15 GHz. In their apparatus, the laser excitation has taken place inside a microwave cavity, either before or after the microwave field pulse is switched on, whose length has typically been from a few tenths to *circa* $1 \mu\text{s}$. The various fields—laser for state preparation, microwave for interaction, and ramped static field for (state) “selective field ionization” (SFI) detection [32,33]—applied to the atoms are all pulsed sequentially in time.

The method [34–36] used in the present work with Rb Rydberg atoms in a thermal beam shares some common ground with both of the methods just mentioned. Figure 1 shows the part of the experimental setup that is important for the present discussion. A thermal beam of Rb atoms with density near 10^9 atoms/cm³ was produced by a two-stage oven source [typical oven (nozzle) temperature of 450 (590) K] and collimator not shown in the figure. The atoms then flew with a most-probable velocity near 410 m/s through spatially separated laser excita-

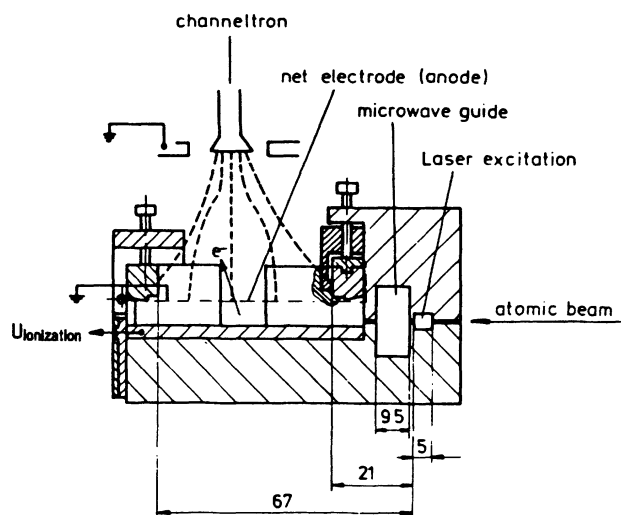


FIG. 1. Side view of the experimental block, most of which is made of gold-plated copper. It was kept at 77 K to minimize the influence of thermal, blackbody photons. The laser excitation, microwave interaction, and selective-field-ionization detection regions are all spatially well separated from each other. The timing of the laser-light pulse, the microwave pulse, and the field ramp was controlled by a pulse generator and delay-line circuitry linked to a laboratory microcomputer. Dimensions shown are in millimeters.

tion, microwave interaction, and ramped-static-field, SFI-detection regions. These are all part of an experimental block whose temperature could be varied. To reduce the effects of blackbody-radiation-induced transitions [27,37] among the Rydberg states, the temperature was fixed at 77 K for the experiments reported in this paper. The pressure was typically below the low 10^{-6} Torr range in the interaction region.

A. Laser excitation

With use of up to 10 mW of near-uv radiation obtained from an intracavity-doubled, rhodamine 6G cw ring-dye laser operating with a typical bandwidth of 1 MHz, we could excite ground-state ${}^4\text{Rb}(5s)^2S_{1/2}$ atoms (both the $A=85$ and 87 isotopes were present in natural abundance) directly to ${}^4\text{Rb}(np)^2P_J$ Rydberg states with n in the range 40–135. Because they produced the strongest signals, we usually used the $nP_{3/2}$ states laser excited from the $F=3$ hyperfine level of the ${}^{85}\text{Rb}$ ground state. The hyperfine structure in the high-lying p states was unresolved. The continuous laser radiation, linearly polarized parallel to the atomic beam axis, was sent through an electro-optic switch opened for $6\ \mu\text{s}$ every $350\ \mu\text{s}$ and was weakly focused at the center of the laser excitation region in the experimental block. This prepared a spatially small group of Rydberg atoms. The microwave field described next was switched on only after every second laser pulse. For the other laser pulses, the microwave field was not switched on.

B. Microwave interaction region

After about $20\ \mu\text{s}$ the center of a laser-excited group of atoms drifted into the center of the microwave interaction region, which had been machined to the dimensions of “ M -band” waveguide ($1.905\times 0.953\ \text{cm}^2$) into the copper experimental block (subsequently gold coated). Slit-shaped, 1-mm-high openings allowed for atomic beam transport with minimal perturbation of the microwave field. The thermal velocity spread of the beam and the $6\text{-}\mu\text{s}$ duration of the laser excitation pulse were small enough that the group of atoms stayed entirely within the waveguide for interaction times used in the present study. For frequencies between the calculated cutoff at $\nu_{1,0}=7.874\ \text{GHz}$ and the calculated onsets of the higher-order $\text{TE}_{2,0}$ and $\text{TE}_{0,1}$ modes at $\nu_{2,0}=15.748\ \text{GHz}$ and $\nu_{0,1}=15.740\ \text{GHz}$, respectively, the waveguide supported only the $\text{TE}_{1,0}$ fundamental mode, whose linear polarization vector was parallel to the atomic beam direction.

The microwave power delivered to the waveguide interaction region originated from the unamplified output of a Systron-Donner Model 1720, 0.05–18 GHz synthesizer, whose unlevelled output power at the fundamental frequency could reach as high as +18 dBm (63 mW) while the power at higher harmonics and in broadband noise remained at least $-50\ \text{dBc}$ (i.e., 50 dB below the carrier). A laboratory microcomputer was used to control both its power and frequency, as well as to control other devices for data collection. Because previous studies [11,12,34] have shown the important effects on Ryd-

berg atoms of appreciable amounts of superimposed broadband noise from, e.g., a microwave amplifier or of a second driving frequency [20,21,36,38] superimposed with a harmonic driving frequency, the low-noise and low-harmonic content of the synthesizer were important for the relatively long, up to $5\ \mu\text{s}$, interaction times used in the present experiments.

The microwave power was transported from the source into the vacuum apparatus through several meters of low-loss coaxial cables and connectors, a coaxial feedthrough, and another meter or so of coaxial cable. Near the experimental block was a transition from coaxial cable to M -band waveguide. The power was finally dissipated beyond the waveguide interaction region in a tapered, lossy waveguide termination inserted into the waveguide inside the vacuum system.

Outside the vacuum system, a coaxial directional coupler was used to sample a portion of the incident power for monitoring with a Marconi Model 6910 power sensor and Model 6950 power meter. An Eyal Microwave Industry Model AR-5360-XX microwave SPST pin-diode coaxial switch was used to send temporal pulses of microwaves to the interaction region. The measured rise and fall times were approximately 6 ns, which at, e.g., 12 GHz, corresponds to a rise and fall of about 70 microwave oscillations. The duration of the “flat top” of the pulse could be varied in steps of 1 ns from approximately 10 ns to longer than $20\ \mu\text{s}$, although the maximum duration used in these experiments was $5\ \mu\text{s}$.

Because of the nonideal properties of real microwave components, the only reliable way to determine the actual microwave field strength experienced by the atoms for a given sampled power measurement was to use the atoms themselves as a probe [8,39,40]. Using the same experimental field-calibration method as was reported by Sirko, Buchleitner, and Walther [40], where the field-calibration accuracy was estimated to be $\pm 3\%$, we carried out 15 *in situ* calibrations using two-photon Rabi-nutation measurements for $\text{Rb } nP_{3/2} - (n+1)P_{3/2}$ transitions at frequencies between 8.8672 ($n=74$) and 16.988 GHz ($n=60$). The neighboring calibration frequencies were separated by 0.4–0.8 GHz. Though the two highest calibration frequencies were above $\nu_{2,0}$ and $\nu_{0,1}$ onsets near 15.75 GHz, their (power) $^{1/2}$ -to-field-amplitude calibration values were comparable to those obtained below the calculated onsets for these higher-order modes. This suggests that above their onsets, at least near these calibration frequencies, there was no serious amount of scattering into these modes in our system.

C. Detection with SFI

About $82\ \mu\text{s}$ after the start of each laser pulse, which was sufficient time for the laser-excited atoms to fly under the field of view of the channeltron electron multiplier in the detection region shown in Fig. 1, a voltage decreasing approximately linearly in time over about $20\ \mu\text{s}$, from 0 V toward typically $-100\ \text{V}$, was applied to the bottom half of a parallel-electrode capacitor. The upper electrode 0.6 cm away was a fine, stretched wire mesh maintained at ground potential. Therefore, the typical slew rate during the field increase was $8.3\ \text{V/cm}\ \mu\text{s}$. For this rate and for

the value of n studied in the present experiment, $n = 84$, the ramped-static-field ionization of the $\text{Rb}(np)^2P_{3/2}$ atoms produced the well-known [32,33] “adiabatic” peak, at relatively lower field strengths, and the “diabatic” peak(s), at relatively larger field strengths. The arrival time distribution for the electrons detected by the channeltron multiplier during a detection time gate of up to about $20 \mu\text{s}$ followed the variation in ionization probability along the field ramp. The peak count rate for the channeltron was kept below several tens of kHz to avoid pulse saturation effects.

During the alternate laser pulses when the microwaves were not switched on, the total number of electron counts in a comparable time-gated detection window, corresponding to ramped electric-field values of “zero” (i.e., stray-field dominated) to the peak value of about 166 V/cm was a measure of the laser-excited Rb np -Rydberg state population. Let us call this signal $S(\text{mw off})$.

During the interleaved set of alternate laser pulses when the microwaves were switched on, the total number of electron counts in the same detection window was a measure of the surviving number of Rb atoms that had been laser excited but had not been ionized by the microwave electric field. Let us call this signal $S(\text{mw on})$. Following customary usage [2,7], we use “ionization” with quotation marks to mean true ionization (excitation into the continuum) plus excitation bound levels above n_c , a cutoff value of n .

D. Determination of the n cutoff and stray electric-field amplitudes

We estimated a value of n_c near 135 as follows. In an auxiliary spectroscopic study in the same apparatus of the uv laser excitation of the Rb $5s$ - np transitions, but with the microwave field switched off, we observed no identifiable np signal for $n \gtrsim 135$. From the well-known formula $n_{\text{eff}}^4 F = \frac{1}{16}$ a.u. for the static-field ionization threshold for low- $|m|$ states of nonhydrogen Rydberg atoms, where $n_{\text{eff}} = (n - \delta)$ is the effective principal quantum number for given values of n and the quantum defect δ , $n_c \simeq 135$ is consistent with a stray static electric field of approximately 1 V/cm in the narrow (about 1-mm wide) channels traversed by the Rb atoms in the experimental block.

However, it is most important to know what the value of stray field could be where the Rb atoms interacted with the microwave field. Because the 0.95-cm width of the M -band waveguide was about 10 times larger than that of the narrow channels mentioned above, we expect that the stray field in the microwave interaction region was at least ten times smaller. Moreover, we were able to confirm this by carrying out numerical simulations of the influence of a static electric field on the two-photon Rabi nutations we used to calibrate the microwave electric-field amplitude. Specifically, the simulations for the two-photon transition $70P_{3/2}$ - $71P_{3/2}$ showed that the presence of a stray electric field $F_s > 0.04 \text{ V/cm}$ in the microwave interaction region would result in experimentally observable phenomena such as a frequency shift or partial smearing in the two-photon Rabi nutations. We

did not observe such effects. A value $F_s = 0.04 \text{ V/cm}$ determines a cutoff value of n in the microwave interaction region of $n'_c \simeq 300$.

Calculations show that the Rb atoms interacting with a microwave field having amplitudes of interest in the present work leads to a broadening of the highly excited levels that can be bigger than their separations. As an example, let us consider a 9.2-GHz microwave field with electric amplitude 2.2 V/cm and the one-photon microwave transition between states $148S$ and $152P$. (Energetically, this would be the result of the transitions between the 37th and 38th quasidegenerate states [17] above an atom initially in the $84P$ Rydberg state; i.e., the states lying, respectively, 37 and 38 photon energies above $84P$.) The angular frequency Ω_R (in a.u.) of the one-photon Rabi nutations is almost equal to the separation ΔE (in a.u.) of the Rb atomic levels $151P$ and $152P$. For comparison, the calculated energy shift of the Rb $152P$ state caused by the quadratic Stark shift in a $F_s = 0.04 \text{ V/cm}$ field is smaller than $\Delta E/20$. These results suggest that the influence of stray electric fields in the microwave interaction region on Rb atoms in states up to and exceeding n_c was much smaller than that of the microwave field itself, whose excellent long-term coherence properties were demonstrated by the two-photon Rabi nutations used to calibrate its amplitude.

E. Definition of the microwave ionization signal

The ratio $P = [S(\text{mw off}) - S(\text{mw on})]/S(\text{mw off})$ gives the microwave “ionization” probability, which was collected and averaged for an equal number of laser pulses for microwaves off and on, for a given set of parameters: initial n value, microwave frequency, field amplitude, and pulse length.

The experimental conditions were such that the “dark” counting-rate (i.e., background pulses from the channeltron or the rest of the detection electronics chain) contribution to $S(\text{on})$ and $S(\text{off})$ was much smaller than $S(\text{off})$. One may easily show that as the microwave power increased from a very small value, where P was consistent with 0, to a value large enough to “ionize” all the laser-excited atoms, where P was consistent with 1, the counting-statistics-induced uncertainty ΔP in the microwave “ionization” probability should be largest when P is small and drop by the factor of $\sqrt{(1-P)/2}$ as P rises toward 1. Hence, we expect the low-“ionization”-probability data to be noisier than the high-“ionization”-probability data; this is consistent with our observations.

III. RESULTS

We chose to collect data for particular frequency ranges that fulfilled two conditions: (i) the interval included a frequency at which the field was calibrated with a two-photon Rabi-nutation measurement [40]; and (ii) the measured variation of the microwave power reflected from the various imperfectly matched microwave components was very small over a given frequency interval, usually less than 20 MHz.

Before moving on to the amplitude-calibrated, frequency-dependence data, Fig. 2 shows how the “ion-

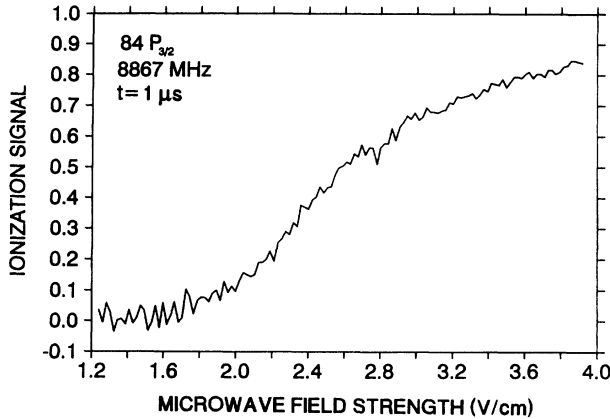


FIG. 2. The amplitude dependence of the microwave “ionization” probability for Rb $(84p)^2P_{3/2}$ atoms, for a $1\text{-}\mu\text{s}$ interaction time. For the frequency shown in the inset, the field amplitude was calibrated absolutely to about $\pm 3\%$ with use of a two-photon Rabi-nutation measurement between the $n=74$ and 75 $^2P_{3/2}$ levels. As is explained in the text, the scaled frequencies $\Omega_{sp} \approx 1.45$ and $\Omega_{pd} \approx 2.47$. (For completeness we also give the value $\Omega_{pp} \approx 0.73$.)

ization” probability varies with the calibrated microwave amplitude for a given initial state, interaction time, and frequency. We mention that the shape of this curve is typical; in the present study, we have observed such ionization curves to rise smoothly, without multiple thresholds, steps, or “bumps” between “ionization” probabilities of 0 and 1. Moreover, Fig. 2 clearly shows, as expected (see Sec. II E), that the counting-statistics-induced jitter in the curve decreases as the plotted ionization signal rises from 0 to 1.

Figures 3–6 show one or two curves each for the frequency dependence of the microwave “ionization” probability that were obtained under calibrated conditions for Rb atoms prepared in the $84P_{3/2}$ state. In the inset or caption for each figure are relevant details, such as the interaction time and which transition and frequency were used to obtain the given and calibrated field amplitude. Typically, 256 frequency steps were used to cover each interval.

The interaction times shown in these figures, 1 and $5\ \mu\text{s}$, were chosen to be shorter than the calculated time-of-flight limitations mentioned in Sec. II, but long enough for the atoms to resolve frequency differences small compared to the range covered in each scan. Because the 6-ns rise and fall of the microwave field was negligible on this timescale, for the purposes of the following estimate we may approximate the microwave pulse shape as square. (Note, however, that the *circa* 70-field-oscillation rise and fall of the microwave field was not at all sudden for the atoms; any theoretical modeling of the quantal evolution should account for this slow rise and fall of the field.)

The Fourier transform of a temporal, rectangular pulse of microwaves of frequency ν that lasts T seconds is a *sinc* function of frequency whose central lobe at frequency ν has a base width of $\Delta\nu = T^{-1}$ Hz. For $t = 1$ or $5\ \mu\text{s}$, respectively, this corresponds to $\Delta\nu = 1$ or 0.2 MHz.

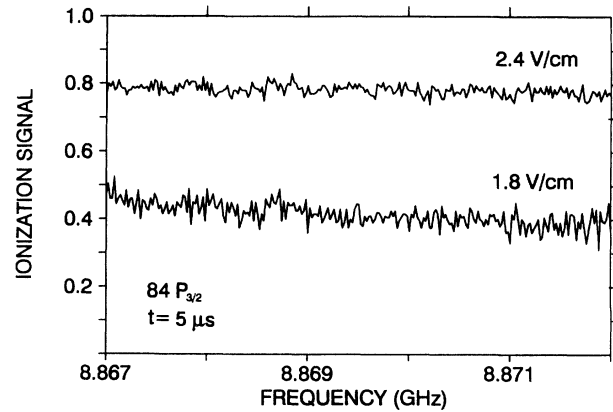


FIG. 3. The frequency dependence over a $\Delta\nu = 5\text{-MHz}$ interval ($\Delta\nu/\nu \approx 5.6 \times 10^{-4}$) for Rb $(84p)^2P_{3/2}$ atoms for two different microwave amplitudes. (The scaled amplitudes are $n_{\downarrow}^4 F = 0.0154$ and 0.0205 for the lower and upper curves, respectively. See the text for a discussion of the scaled amplitude.) The field amplitude scale was calibrated absolutely to about $\pm 3\%$ with use of a two-photon Rabi-nutation measurement between the $n=74$ and 75 $^2P_{3/2}$ levels at 8.8672 GHz. As is explained in the text, the scaled frequencies $\Omega_{sp} \approx 1.452$ and $\Omega_{pd} \approx 2.472$. (For completeness we also give the value $\Omega_{pp} \approx 0.73$.) The microwave pulse length was $5\ \mu\text{s}$ for both curves.

These bandwidths may be taken to be lower limits for the frequency resolution in each case. Physically relevant information about how long the atoms actually could interact coherently with the microwave field was obtained from the two-photon Rabi-nutation measurements [40] used to calibrate the microwave amplitudes in each case. We observed that the contrast of the Rabi-nutation oscil-

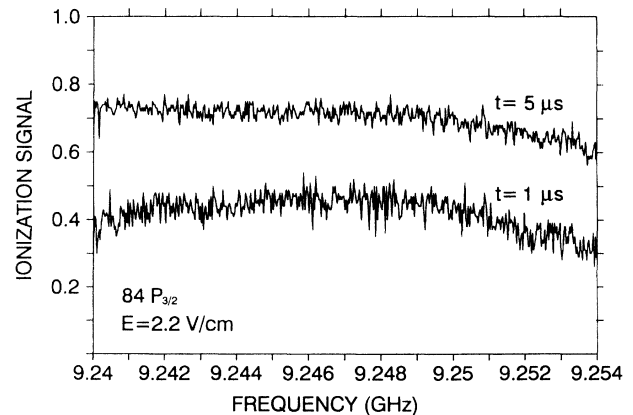


FIG. 4. The frequency dependence over a $\Delta\nu = 14\text{-MHz}$ interval ($\Delta\nu/\nu \approx 1.5 \times 10^{-3}$) for Rb $(84p)^2P_{3/2}$ atoms for two different microwave pulse lengths, both for a field amplitude of $2.2\ \text{V/cm}$. (The scaled amplitude is $n_{\downarrow}^4 F = 0.0188$. See the text for a discussion of the scaled amplitude.) The field amplitude scale was calibrated absolutely to about $\pm 3\%$ with use of a two-photon Rabi-nutation measurement between the $n=73$ and 74 $^2P_{3/2}$ levels at 9.2479 GHz. As is explained in the text, the scaled frequencies $\Omega_{sp} \approx 1.514$ and $\Omega_{pd} \approx 2.578$. (For completeness we also give the value $\Omega_{pp} \approx 0.756$.) Notice that the “ionization” probability increases with increasing pulse length, with all other conditions the same.

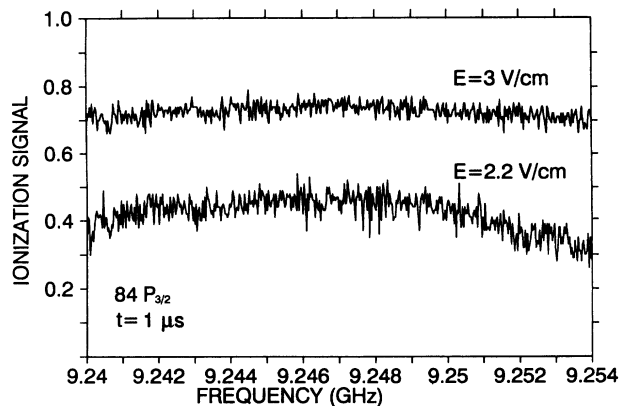


FIG. 5. The frequency dependence over a $\Delta\nu=14$ -MHz interval ($\Delta\nu/\nu \approx 1.5 \times 10^{-3}$) for the Rb $(84p)^2P_{3/2}$ atom, for two different microwave amplitudes. (The scaled amplitudes are $n_*^4 F = 0.0188$ and 0.0256 for the lower and upper curves, respectively. See the text for a discussion of the scaled amplitude.) The field amplitude scale was calibrated absolutely to about $\pm 3\%$ with use of a two-photon Rabi-nutation measurement between the $n = 73$ and 74 $^2P_{3/2}$ levels at 9.2479 GHz. As is explained in the text, the scaled frequencies $\Omega_{sp} \approx 1.514$ and $\Omega_{pd} \approx 2.478$. (For completeness we also give the value $\Omega_{pp} \approx 0.756$.) The microwave pulse length was $1 \mu\text{s}$ for both curves.

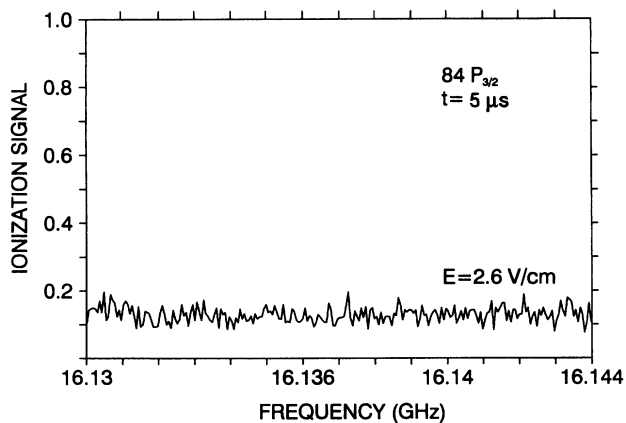


FIG. 6. The frequency dependence over a $\Delta\nu=14$ -MHz interval ($\Delta\nu/\nu \approx 8.7 \times 10^{-4}$) for Rb $(84p)^2P_{3/2}$ atoms exposed to a $5\text{-}\mu\text{s}$ pulse length and a 2.6-V/cm field amplitude. (The scaled amplitude $n_*^4 F = 0.0222$. See the text for a discussion of the scaled amplitude.) The field amplitude scale was calibrated absolutely to about $\pm 3\%$ with use of a two-photon Rabi-nutation measurement between the $n = 61$ and 62 $^2P_{3/2}$ levels at 16.1367 GHz. As is explained in the text, the scaled frequencies $\Omega_{sp} \approx 2.642$ and $\Omega_{pd} \approx 4.498$. (For completeness we also give the value $\Omega_{pp} \approx 1.320$.) Notice that for the same $5\text{-}\mu\text{s}$ pulse length, the “ionization” probability for this curve, at the larger driving field of 2.6 V/cm , is lower than that for the upper curve in Fig. 4, taken at the smaller driving field of 2.2 V/cm . As is explained in the text, these and other data may be used to establish that the data shown in Figs. 2–6 are in the regime of scaled frequencies above 1.

lations decayed with increasing interaction time. Typical values for the decay constant were from 1 to $2 \mu\text{s}$, which correspond to coherent-interaction bandwidths of 1 and 0.5 MHz , respectively. Because all the bandwidths mentioned in this paragraph are smaller than the frequency intervals spanned in Figs. 3–6, these intervals are physically interesting for the 1 - and $5\text{-}\mu\text{s}$ interaction times.

We now say a few words about the data recorded in each of the Figs. 3–6, but the interpretation of these data will be given in the next section. Figure 3 compares over a 5-MHz interval near the lower end of the experimentally accessible frequency range the “ionization” signals for two different microwave amplitudes, both taken with $5\text{-}\mu\text{s}$ interaction time. The jitter in each trace around an approximately constant signal level is consistent with what would be expected from counting statistics. Moreover, this jitter is on a frequency scale at least three times finer than what would be expected from the frequency resolution estimated above, $\Delta\nu = 0.2 \text{ MHz}$. One may notice that the “ionization” probability is higher at the higher microwave amplitude but that there is no physically important frequency-dependent variation of these signals greater than about 10% in the lower trace, or about half this amount in the upper trace.

Over a 14-MHz interval of frequencies a bit higher than those shown in Fig. 3, Fig. 4 compares “ionization” signals for two different interaction times, both taken with an amplitude of 2.2 V/cm . Again, the fine-scale variations are not outside those expected from counting statistics, but there is some gross behavior worthy of comment. First, the “ionization” probability for $5 \mu\text{s}$ is appreciably larger than that for $1 \mu\text{s}$. This may be contrasted to the behavior reported by Gallagher and co-workers [29] for the 15-GHz “ionization” of Li and Na atoms prepared in nd states with some n values in the range $33\text{--}67$; their observed microwave “ionization” threshold fields were described as unchanged for pulse lengths between 300 ns and $1 \mu\text{s}$. Second, there is a smooth variation with frequency for both traces shown in Fig. 4, more so for the lower one. The falloff of both curves at the upper frequency end is likely due to the frequency-dependent, voltage standing-wave ratio (VSWR)-induced variation of the microwave amplitude beginning to come into play. However, unlike the upper curve, the lower curve also falls off slightly at the lower frequency end.

For the same 14-MHz frequency interval shown in Fig. 4, Fig. 5 compares for a fixed, $1\text{-}\mu\text{s}$ interaction time the “ionization” signals for two different microwave amplitudes; the lower curve is repeated from Fig. 4. Once again, the fine-scale variations in both curves are not outside those expected from counting statistics, but the mean behavior of the upper curve is noticeably flatter than for the lower curve. As was the case in Fig. 3, the ionization probability is larger for the higher microwave amplitude.

Figure 6 shows over a 14-MHz interval the “ionization” probability for a microwave amplitude of 2.6 V/cm and an interaction time of $5 \mu\text{s}$; this interval covered the highest frequencies studied in the present experiments. Over this interval the signal is flat within the variations expected from counting statistics. One should notice,

however, that the mean 13% “ionization” probability at 2.6 V/cm for these frequencies near 16 GHz is *lower* than that for the data in Fig. 4 taken at the lower 2.2-V/cm microwave amplitude and lower frequency range: i.e., at a higher frequency, the “ionization” probability is lower than that at a lower frequency with a higher amplitude.

IV. DISCUSSION OF RESULTS

The data shown in Figs. 3–6 display no sharp, physically important frequency dependence of the microwave “ionization” probability for Rb $84P_{3/2}$ states over 5–14 MHz intervals around a few frequencies ranging from 8.87 to 16.14 GHz. We cannot rule out that physically important, sharp structure might be present for experimental conditions we did not investigate, but the present survey establishes that if such structure exists, it is not ubiquitous for Rb Rydberg atoms.

We now focus on other interesting aspects of the present data. Experiments and theory on the microwave “ionization” of excited hydrogen atoms have found six different regimes [5,7] of dynamical behavior for different ranges of the scaled frequency [41] that, for generality, we shall call Ω . For the classical hydrogen atom, $\Omega = \omega/\omega_{\text{at}}$, where ω is the angular driving frequency and ω_{at} is the atomic “Kepler” frequency, which scales with principal action I_0 as I_0^{-3} . For quantized principal action $I_0 = n_0 \hbar$, by Bohr’s correspondence principle ω_{at} is given very closely by the mean of the $n_0 \rightarrow (n_0 \pm 1)$ transition frequencies, and $\Omega_{\text{H}} = n_0^3 \omega$.

For nonhydrogenic Rydberg atoms, by which we mean those excited into and driven among states at least some of which have quantum defects δ for which $\delta(\text{mod } 1)$ is not much smaller than 1, it is not obvious how to generalize the notion of ω_{at} . If $n_* = (n_0 - \delta_0)$ is the effective principal quantum number for the initial, laser-excited $n_0^2 P_{3/2}$ state with quantum defect δ_0 , might one adopt a hydrogenlike expression $\Omega_{pp} \approx n_*^3 \omega$, or should it be something else? [The subscript *pp* indicates that ω_{at} is given by the mean of the $n_0^2 P_{3/2} \rightarrow (n_0 \pm 1)^2 P_{3/2}$ frequency splittings.] The quantum defects for the high-lying $n^2 S_{1/2}$, $n^2 P_{3/2}$, and $n^2 D_{5/2}$ states of Rb Rydberg atoms are 3.1312, 2.6418, and 1.3464, respectively [42,43]. If only the Rb *S* and *P* states play a dominant role in the microwave “ionization” of laser-excited Rb $n_0^2 P_{3/2}$ states, then one might take for ω_{at} the $n_0^2 P_{3/2} \rightarrow (n_0 + 1)^2 S_{1/2}$ splitting or the average of the $n_0^2 P_{3/2} \rightarrow (n_0 + 1)^2 S_{1/2}$ and $n_0^2 P_{3/2} \rightarrow n_0^2 S_{1/2}$ transitions. We shall call this average ω_{sp} . In that case Ω would be approximated by $\Omega_{sp} = \omega/\omega_{sp} \approx 2\Omega_{pp}$. However, for Rb atoms there is also another possible choice of the scaled frequency connected with the $n_0^2 P_{3/2}$ and $(n_0 - 1)^2 D$ states. In that case $\Omega_{pd} = \omega/\omega_{pd} \approx 3.3\Omega_{pp}$.

Two microwave “ionization” experiments [2,24] with excited hydrogen atoms have shown that for a given interaction time and for an n cutoff n_c lying far above the initial n_0 value, the classically scaled microwave amplitudes $\mathcal{F}(10\%)$ needed to produce a 10% “ionization” probability rise, on average, with increasing Ω_{H} when Ω_{H} exceeds about 1–2. For hydrogen atoms, the scaled amplitude \mathcal{F} is given by the ratio of the microwave electric

amplitude F to the Coulomb electric field binding the electron to the proton in the Bohr atom (circular orbit) with initial level n_0 : $\mathcal{F}_{\text{H}} = n_0^4 F$. Except near resonances of various kinds, where the behavior can be complicated [2,5,7,44], the experimental $\mathcal{F}_{\text{H}}(10\%)$ values lie increasingly above their classically computed counterparts as Ω_{H} rises. Indeed, this observed increasing quantal stability, on the “average,” with increasing Ω_{H} in the high-frequency regime confirmed prior predictions [45,46] of this effect that had been based on the theory of dynamical localization and quantal numerical calculations [47].

Let us then take the rise (on average) of the \mathcal{F} values, either for 10% or other “ionization” probabilities, with Ω increasing above some value to be a “fingerprint” for the enhanced stability due to dynamical localization. Let us define the scaled amplitude for Rb Rydberg atoms to be $\mathcal{F}_{\text{Rb}} = n_*^4 F$. An experimental study carried out with the same apparatus used in the present experiments, and whose results have been published elsewhere [35,48], investigated at various driving frequencies the n dependence of the microwave amplitudes needed to produce given values of the “ionization” probability. Experimental data [35,48] for the 8.867-GHz microwave “ionization” of Rb nP atoms, with values of n in the range 55–95, show a nearly linear rise of the $\mathcal{F}_{\text{Rb}}(10\%)$ values when n either decreases below about 59 or increases above about 67. That is, there is a local minimum at $\mathcal{F}_{\text{Rb}}(10\%) \approx 0.005$ for values of n between about 59–67. This rough V shape for $\mathcal{F}_{\text{Rb}}(10\%)$ vs either Ω_{sp} or Ω_{pd} recalls the observed and theoretically understood behavior of $\mathcal{F}_{\text{H}}(10\%)$ vs Ω_{H} for excited hydrogen atoms, for which the bottom of the roughly V-shaped curve occurs for $\Omega_{\text{H}} \approx 0.8$ [2,7,9,24].

Let us assume, therefore, that the rise in $\mathcal{F}_{\text{Rb}}(10\%)$ for $n \gtrsim 63$ at 8.867 GHz signals the entrance into the high-frequency regime (called Regime-*V* in Refs. [5,7], or the localized regime in Refs. [47] and [9]). For $n = 63$ and these driving frequencies, $\Omega_{sp} \approx 0.6$ and $\Omega_{pd} \approx 1.0$, respectively; whereas, $\Omega_{pp} \approx 0.3$. The fact that the bottom of the V-shaped curve for H occurs for $\Omega_{\text{H}} \approx 0.8$, which is between the values just given for Ω_{sp} and Ω_{pd} , indicates that the *S* and *D* states might be equally important in the ionization of Rb atoms. (However, $\Omega_{pp} \approx 0.3$ is not close to $\Omega_{\text{H}} \approx 0.8$.) For this reason, in the description of our experiments we will use both scaled frequencies Ω_{sp} as well as Ω_{pd} . It is important to point out [36], however, that there is also no simple accord between the scaled amplitudes for hydrogen and Rb, \mathcal{F}_{H} , and \mathcal{F}_{Rb} , respectively, when $\Omega_{\text{H}} \approx \Omega_{sp}$ or Ω_{pd} (or, for that matter, when $\Omega_{\text{H}} \approx \Omega_{pp}$). It seems that the interleaved quantum-defect-shifted states in Rb Rydberg atoms cause the scaled amplitude \mathcal{F}_{Rb} for, say, 10% “ionization” of Rb atoms to be much lower than the corresponding \mathcal{F}_{H} value, even when the n values and driving frequency are the same. It is equally important to mention that for the n values and frequency ranges covered in the present paper, the Rb microwave “ionization” curves [35] that record the “ionization” probability for fixed n and driving frequency vs the microwave amplitude are smooth and rise monotonically, without “steps;” see, e.g., Fig. 2.

For the present experimental conditions we have not observed double “ionization” thresholds, such as the “nonhydrogenic” thresholds and “hydrogenlike” thresholds previously observed with other Rydberg atoms, e.g., He [8,25], Li, and Na [29]. However, these experiments studying other Rydberg atoms have, thus far, used microwave frequencies that were always significantly below the $n \rightarrow (n \pm 1)$ frequency splittings for the initial state. For the present experimental study of Rb Rydberg atoms, we believe that the data displayed here are in the high-frequency regime. Nevertheless, more experimental and theoretical work is needed for a clear understanding of frequency and amplitude scalings for nonhydrogenic atoms.

The captions for Figs. 3–6 show the values of Ω_{sp} and Ω_{pd} for the middle of each frequency range. (In parentheses, for completeness, the corresponding value of Ω_{pp} is given.) From those captions, one may see that the data cover small intervals in a range between $\Omega_{sp} = 1.45$ – 2.64 , or $\Omega_{pd} = 2.47$ – 4.50 ($\Omega_{pp} = 0.73$ – 1.32). These scaled frequencies are comparable to those for which the computed “ionization” probability obtained from the numerically iterated quantum-Kepler-map [47,16] model for the microwave “ionization” of one-dimensional hydrogen atoms produced [16] “. . . huge fluctuations, . . . which persist down to a very fine frequency scale and have a qualitatively random nature.”

V. CONCLUSIONS

The computed fluctuations mentioned at the end of the last paragraph were one of the motivating factors for the present measurements. The authors of Ref. [16] “. . . argued that such [computed] fluctuations are a counterpart of the mesoscopic fluctuations of solid-state physics, and that similar fluctuations should be expected any time, when some classical chaotic diffusive process is quantum-mechanically suppressed by dynamical localization.” If one views the problem of the interaction of Rydberg atoms with strong microwave fields as a transport problem, where for microwave “ionization” the emphasis is on transport out of the initial state to much higher-lying states—eventually, the continuum—it is interesting to see how much basis there is for the analogy [16,19] between the mesoscopic conductance fluctuations (see Harris, Pals, and Woltjer [49] for a review) in “quantum wires” in solid-state physics and this problem in strong-field atomic physics. In the microwave-driven atom, the transport is either among the atomic states highly perturbed by the field [50], or, in the framework of the “photonic localization” theory [47], among the photonic states separated in energy by the microwave photon energy. The minimum number of such photonic states separating $n = 84$ and $n_c \simeq 135$ ranges from about 35 for Fig. 3 to about 19 for Fig. 6. These “photonic states” might be the analog of the mesoscopic scattering sites.

In the solid-state physics of “mesoscopic” semiconductor devices [49], a number of criteria must be satisfied for the conductance fluctuations to be observed as a large effect. The fluctuations are a result of quantal interferences, and these require coherence. If there is too much

averaging or smearing out of the phases associated with quantal amplitudes, the fluctuations are washed out. The *inelastic mean free path* sets an important length scale for the washing out of phases associated with transport in solid-state devices. The *elastic mean free path* sets another length scale. Generally speaking, mesoscopic fluctuations are observed at very low temperatures in “quantum wires” whose lengths *circa* 1–10 μm are less than the inelastic mean free path but not short compared to the elastic mean free path. (Otherwise “ballistic” electron transport [49] is possible.) The transverse dimensions are much smaller, *circa* hundreds of \AA or less. Viewed as a boundary-value problem, this means that the transverse-mode quantum numbers are small, which obviously leads to a lower total local mode density, and less “averaging.”

Returning to the present case of atoms in strong driving fields, a recent paper [17] using numerical computations and analysis compared the iterated quantum-Kepler-map solutions to solutions of the time-dependent Schrödinger equation in 1+1 dimensions (1 in space plus time) carried out for the same scaled frequency and amplitude. This study led the authors of [17] to conclude for high scaled frequencies (on the order of 20) that the wild fluctuations [16] on a fine frequency scale produced by solutions of the iterated quantum-Kepler map were not physical but were an artifact of the discrete map, introduced by a fixed number of map iterations not corresponding to a fixed time duration (i.e., number of field oscillations) for each basis element in the map. They conjectured that the same effect persists when the scaled frequency drops, e.g., as low as 2. Because this “time-distortion” effect grows with n as n^3 , it is particularly troublesome [17] for basis elements corresponding to extremely weakly bound states, where $n \rightarrow \infty$. The complications for quantized maps produced by the time-distortion effect were subsequently discussed elsewhere [51,52]; p. 3978 of [52] states, “*Clearly a theory avoiding this problem while maintaining the description in terms of the map would be very valuable, but, unfortunately, does not exist so far.*”

Reference [17] argues that the results of this time-distortion effect are that resonances involving very high-lying basis elements of the map have widths that are less than the separation between neighboring states. When various resonances interfere, particularly when very high-lying states are involved, huge fluctuations occur as the frequency parameter is varied for the map. For the continuous system modeled by solutions of the time-dependent Schrödinger equation in (1+1) dimensions, Ref. [17] further argues that the resonances involving very high-lying states have widths that *exceed* the separation between neighboring high-lying states and cause the sharp frequency-dependent structure to be smeared out.

If the (spatial) “dimensionality” of the actual atomic system is higher than the above case (or, said another way, if the local density of participating states is higher), one would naturally expect more smearing out, just as it occurs when one goes from the quasi-one-dimensional, solid-state “wire” to the case of three-dimensional bulk matter. The actual dimensionality of the multielectron Rb atom is obviously higher than for the one-electron

“real” hydrogen atom, and even more so compared to the $(1+1)$ dimensional, model hydrogen atom. Moreover, because of degeneracy, the field-free atomic hydrogen frequencies depend only on the principal quantum number n_0 . Because the nonzero quantum defects of the Rydberg Rb atom break this degeneracy, it is a higher dimensional system than a hydrogen atom. Nevertheless, the observation of the enhanced stability due to dynamical localization in the microwave ionization of Rb $n^2P_{3/2}$ states [35,48] may indicate that at least some of the behavior of the Rb atoms could be modeled with only a few degrees of freedom.

The present experimental data show no fine-scale structure in the frequency dependence of the microwave “ionization” of Rb Rydberg atoms for parameters for which a good case can be made that the effective scaled frequency

is above 1. One should expect that structure will become visible over wider frequency intervals, but this will require a broadband microwave system that is calibrated at a significantly higher number of frequencies than the present one. With such a system one should look forward to probing the frequency dependence over wider ranges as well as to studying the behavior of this system as other important parameters are varied.

ACKNOWLEDGMENTS

P.M.K. appreciates receiving financial support from the Alexander von Humboldt-Stiftung. He is grateful for the hospitality extended by the researchers and staff of the Sektion Physik der Universität München and the Max-Planck-Institut für Quantenoptik.

-
- [1] J. E. Bayfield and P. M. Koch, *Phys. Rev. Lett.* **33**, 258 (1974).
- [2] E. J. Galvez, B. E. Sauer, L. Moorman, P. M. Koch, and D. Richards, *Phys. Rev. Lett.* **61**, 2011 (1988).
- [3] J. E. Bayfield, L. D. Gardner, and P. M. Koch, *Phys. Rev. Lett.* **39**, 76 (1977).
- [4] P. M. Koch, in *Fundamental Aspects of Quantum Theory*, edited by V. Gorini and A. Frigerio (Plenum, New York, 1986).
- [5] P. M. Koch and K. A. H. van Leeuwen (unpublished).
- [6] K. A. H. van Leeuwen, G. v. Oppen, S. Renwick, J. B. Bowlin, P. M. Koch, R. V. Jensen, O. Rath, D. Richards, and J. G. Leopold, *Phys. Rev. Lett.* **55**, 2231 (1985).
- [7] P. M. Koch, L. Moorman, and B. E. Sauer, *Comments At. Mol. Phys.* **25**, 165 (1990); B. E. Sauer, M. R. W. Beller-mann, and P. M. Koch, *Phys. Rev. Lett.* **68**, 1633 (1992), and references therein.
- [8] W. van de Water, S. Yoakum, K. A. H. van Leeuwen, B. E. Sauer, L. Moorman, E. J. Galvez, D. R. Mariani, and P. M. Koch, *Phys. Rev. A* **42**, 572 (1990); S. Yoakum, L. Sirko, and P. M. Koch, *Phys. Rev. Lett.* **69**, 1919 (1992); L. Sirko, S. Yoakum, A. Haffmans, and P. M. Koch, *Phys. Rev. A* **47**, R782 (1993), and references therein.
- [9] J. E. Bayfield, *Comments At. Mol. Phys.* **25**, 213 (1990), and references therein.
- [10] J. E. Bayfield and L. A. Pinnaduwege, *Phys. Rev. Lett.* **54**, 313 (1985); *J. Phys. B* **18**, L49 (1985).
- [11] J. E. Bayfield and D. W. Sokol, in *Advances in Laser Science-III*, Proceedings of the Third International Laser Science Conference, Atlantic City, NJ, 1987, edited by A. C. Tam, J. L. Gole, and W. C. Stwalley, AIP Conf. Proc. No. 172 (AIP, New York, 1988), pp. 326–328.
- [12] J. E. Bayfield and D. W. Sokol, in *Atomic Spectra and Collisions in External Fields*, edited by K. T. Taylor, M. H. Nayfeh, and C. W. Clark (Plenum, New York, 1988), pp. 315–326.
- [13] T. F. Gallagher, *Comments At. Mol. Phys.* **25**, 159 (1990), and references therein.
- [14] R. Blümel and U. Smilansky, *Z. Phys. D* **6**, 83 (1987).
- [15] R. Blümel and U. Smilansky, *J. Opt. Soc. Am. B* **7**, 664 (1990).
- [16] G. Casati, I. Guarneri, and D. L. Shepelyansky, *Physica A* **163**, 205 (1990).
- [17] J. G. Leopold and D. Richards, *J. Phys. B* **23**, 2911 (1990).
- [18] J. G. Leopold and D. Richards, *J. Phys. B* **24**, 1209 (1991).
- [19] G. Casati (private communication).
- [20] L. Moorman, E. J. Galvez, K. A. H. van Leeuwen, B. E. Sauer, A. Mortazawi-M, G. von Oppen, and P. M. Koch, in *Atomic Spectra and Intense Fields*, edited by K. T. Taylor, M. H. Nayfeh, and C. W. Clark (Plenum, New York, 1988), pp. 343–357.
- [21] L. Moorman, E. J. Galvez, B. E. Sauer, A. Mortazawi-M, K. A. H. van Leeuwen, G. v. Oppen, and P. M. Koch, *Phys. Rev. Lett.* **61**, 771 (1988).
- [22] P. M. Koch, L. Moorman, B. E. Sauer, E. J. Galvez, K. A. H. van Leeuwen, and D. Richards, *Phys. Scr.* **T26**, 51 (1989).
- [23] D. Richards, J. G. Leopold, P. M. Koch, E. J. Galvez, K. A. H. van Leeuwen, L. Moorman, B. E. Sauer, and R. V. Jensen, *J. Phys. B* **22**, 1307 (1989).
- [24] J. E. Bayfield, G. Casati, I. Guarneri, and D. W. Sokol, *Phys. Rev. Lett.* **63**, 364 (1989).
- [25] D. R. Mariani, W. van de Water, P. M. Koch, and T. Bergeman, *Phys. Rev. Lett.* **50**, 1261 (1983).
- [26] P. M. Koch, in *Rydberg States of Atoms and Molecules*, edited by R. F. Stebbings and F. B. Dunning (Cambridge University Press, New York, 1983), pp. 473–512.
- [27] T. F. Gallagher, in *Rydberg States of Atoms and Molecules* (Ref. [26]), p. 165–186.
- [28] R. C. Stoneman, D. S. Thomson, and T. F. Gallagher, *Phys. Rev. A* **37**, 1527 (1988).
- [29] T. F. Gallagher, C. R. Mahon, P. Pillet, P. Fu, and J. B. Newman, *Phys. Rev. A* **39**, 4545 (1989); C. R. Mahon, J. L. Dexter, P. Pillet, and T. F. Gallagher, *ibid.* **44**, 1859 (1991).
- [30] U. Eichmann, J. L. Dexter, E. Y. Xu, and T. F. Gallagher, *Z. Phys. D* **11**, 187 (1989).
- [31] Panming Fu, T. J. Scholz, J. M. Hettema, and T. F. Gallagher, *Phys. Rev. Lett.* **64**, 511 (1990); see also M. Nauenberg, *ibid.* **64**, 2731 (1990); T. F. Gallagher, *Mod. Phys. Lett. B* **5**, 259 (1991).
- [32] T. H. Jeys, G. W. Foltz, K. A. Smith, F. G. Kellert, E. J. Beiting, F. B. Dunning, and R. F. Stebbings, *Phys. Rev. Lett.* **44**, 390 (1980).
- [33] F. B. Dunning and R. F. Stebbings, in *Rydberg States of Atoms and Molecules* (Ref. [26]), pp.315–353, see Sec. 9.2b.
- [34] R. Blümel, R. Graham, L. Sirko, U. Smilansky, H. Walther, and K. Yamada, *Phys. Rev. Lett.* **62**, 341 (1989); R. Blümel, A. Buchleitner, R. Graham, L. Sirko, U. Smilan-

- sky, and H. Walther, *Phys. Rev. A* **44**, 4521 (1991).
- [35] M. Arndt, Diplom thesis, Ludwig-Maximilians-Universität München, 1990.
- [36] A. Buchleitner, L. Sirko, and H. Walther, in *Quantum Chaos*, Proceedings of the Adriatico Research Conference and Miniworkshop, International Centre for Theoretical Physics, Trieste, 1990, edited by H. A. Cerdeira, R. Ramaswamy, M. C. Gutzwiller, and G. Casati (World Scientific, Singapore, 1991), pp. 395–408.
- [37] H. Figger, G. Leuchs, R. Straubinger, and H. Walther, *Opt. Commun.* **33**, 37 (1980).
- [38] G. A. Ruff, K. M. Dietrick, and T. F. Gallagher, *Phys. Rev. A* **42**, 5648 (1990).
- [39] W. van de Water, K. A. H. van Leeuwen, S. Yoakum, E. J. Galvez, L. Moorman, T. Bergeman, B. E. Sauer, and P. M. Koch, *Phys. Rev. Lett.* **63**, 762 (1989).
- [40] L. Sirko, A. Buchleitner, and H. Walther, *Opt. Commun.* **78**, 403 (1990).
- [41] J. G. Leopold and I. C. Percival, *Phys. Rev. Lett.* **41**, 944 (1978).
- [42] D. Meschede, *J. Opt. Soc. Am. B* **4**, 413 (1987).
- [43] T. Bergeman (private communication).
- [44] R. V. Jensen, S. M. Susskind, and M. M. Sanders, *Phys. Rev. Lett.* **62**, 1476 (1989).
- [45] D. Shepelyansky, in *Chaotic Behavior in Quantum Systems*, edited by G. Casati (Plenum, New York, 1985), pp. 187–204.
- [46] G. Casati, B. V. Chirikov, and D. L. Shepelyansky, *Phys. Rev. Lett.* **53**, 2525 (1984).
- [47] G. Casati, I. Guarneri, and D. L. Shepelyansky, *IEEE J. Quantum Electron.* **24**, 1240 (1988).
- [48] M. Arndt, A. Buchleitner, R. Mantegna, and H. Walther, *Phys. Rev. Lett.* **67**, 2435 (1991).
- [49] J. J. Harris, J. A. Pals, and R. Woltjer, *Rep. Prog. Phys.* **52**, 1217 (1989).
- [50] N. B. Delone, B. A. Zon, and V. P. Krainov, *Zh. Eksp. Teor. Fiz.* **75**, 445 (1978) [*Sov. Phys. JETP* **48**, 223 (1978)].
- [51] B. V. Chirikov, in *Chaos and Quantum Physics*, Les Houches LII, 1989, edited by M.-J. Giannoni, A. Voros, and J. Zinn-Justin (Elsevier, Amsterdam, 1991), p. 476.
- [52] R. Graham and M. Höhnerbach, *Phys. Rev. A* **43**, 3966 (1991).